

$$\psi = 1 - e^{\epsilon/kT} + \frac{\epsilon}{2kT} \left[ 1 + \frac{4}{\pi} e^{\epsilon/kT} \int_0^\infty e^{-x^2} x^2 dx \right] \sqrt{\epsilon/kT}$$

#### LITERATURE CITED

1. Davis, H. T., S. A. Rice, and J. V. Sengers, *J. Chem. Phys.*, **35**, 2210 (1961).
2. Davis, H. T., and K. D. Luks, *J. Phys. Chem.*, **69**, 869 (1965).
3. Wertheim, M. S., *Phys. Rev. Letters*, **10**, 321 (1963).
4. Thiele, E., *J. Chem. Phys.*, **39**, 474 (1963).
5. Prigogine, I., G. Nicholis, and J. Misguish, *ibid.*, in press.
6. Naghizadeh, J., *ibid.*, **39**, 3406 (1963).
7. Bearman, R. J., *ibid.*, **29**, 1278 (1958).
8. Longuett-Higgins, H. C., and J. P. Valleau, *Molecular Phys.*, **1**, 284 (1956).
9. Hirschfelder, J. O., C. F. Curtiss, and R. B. Bird, "Molecular Theory of Gases and Liquids," Wiley, New York (1954).
10. Lowry, B. A., H. T. Davis, and S. A. Rice, *Phys. Fluids*, **7**, 402 (1964).
11. Broyles, A. A., *J. Chem. Phys.*, **35**, 493 (1961).
12. Percus, J. K., and G. J. Yevick, *Phys. Rev.*, **110**, 1 (1957).
13. Wood, W. W., and J. D. Jacobsen, *J. Chem. Phys.*, **27**, 1207 (1957).
14. Throop, G. J., and R. J. Bearman, *ibid.*, **42**, 2408 (1965).
15. Cook, G. A., "Argon, Helium and the Rare Gases," Interscience, New York (1961).
16. Hougen, O. A., K. M. Watson, and R. A. Ragatz, "Chemical Process Principles," Vol. 2, Wiley, New York (1962).
17. Ikenberry, L. D., and S. A. Rice, *J. Chem. Phys.*, **39**, 1561 (1963).
18. Naghizadeh, J., and S. A. Rice, *ibid.*, **36**, 2710 (1962).
19. Michels, A., and R. O. Gibson, *Proc. Roy. Soc. (London)*, **A134**, 288 (1961); A. Michels, J. V. Sengers, and van der Gulik, *Physica*, **28**, 1216 (1962); A. Michels, J. V. Sengers, and van de Klundert, *Physica*, **29**, 149 (1963); J. V. Sengers, W. T. Bolk, and C. J. Stigter, *Physica*, **30**, 1018 (1964).
20. Rice, S. A., and A. R. Allnatt, *J. Chem. Phys.*, **34**, 2144 (1961).
21. Allnatt, A. R., and S. A. Rice, *ibid.*, **34**, 2156 (1961).
22. Rice, S. A., and P. Grey, "Statistical Mechanics of Fluids," Wiley, New York (1966).
23. Kirkwood, J. G., V. A. Lewinson, and B. J. Alder, *J. Chem. Phys.*, **20**, 929 (1952).

Manuscript received January 18, 1966; revision received April 11, 1966; paper accepted April 22, 1966. Paper presented at A.I.Ch.E. Columbus meeting.

# Flow in Concentric Annuli at High Reynolds Numbers

R. R. ROTHFUS, W. K. SARTORY, and R. I. KERMODE

Carnegie Institute of Technology, Pittsburgh, Pennsylvania

A method is proposed and developed for predicting velocity profiles in smooth, concentric annuli at high Reynolds numbers from the profiles in equivalent tubes. Experimental data for the flow of water in two annuli with diameter ratios of 14.8 and 38.2 at Reynolds numbers up to 226,000 strongly support the predictions. Published data show the method to be successful over a very wide range of diameter ratios.

The problem of flow in noncircular ducts is an old and difficult one. When the motion is turbulent, it is customary to compare the fluid behavior with that in an equivalent tube. The practical problem is to find the proper conditions for comparison.

Concentric annuli are especially interesting noncircular ducts for they have two continuous, easily described boundaries, each exerting uniform but different skin frictions on the fluid. As the diameter ratio passes to its limits, the configuration goes to a tube on one hand and parallel

plates on the other. When an annulus is compared with a tube, it is therefore being compared with another type of annulus rather than an entirely different kind of duct.

Barring unexpected complications, the rules governing flow in a tube have a good chance of applying generally to the portion of an annulus between the radius of maximum fluid velocity and the outer wall. If the rules apply equally well to both the inner and outer parts of the annular duct, both sides of the maximum point can be related to respective equivalent tubes through the same kind of generality.

When the annular flow is entirely laminar, the radius of maximum velocity is such that the comparison with tubular flow can be made by means of straightforward

W. K. Sartory is with Oak Ridge National Laboratory, Oak Ridge, Tennessee.

geometrical transformations (4). It has been demonstrated that the same rules apply to turbulent flow provided the maximum point remains at its laminar position (5). At high Reynolds numbers, however, the maximum point lies appreciably closer to the core than it does in the laminar case (1). Consequently, the appropriate transformations are more complicated. The present work extends the comparison of tubes and annuli to high Reynolds numbers and supports the results with pertinent experimental data.

#### DISTRIBUTION OF SHEARING STRESS

When a fluid of constant properties flows steadily in a uniform, concentric annulus without extraneous forces, the absolute value of the shearing stress at the arbitrary radius  $r$  is

$$\tau g_c = \frac{\Delta p g_c}{L} \left| \frac{r_s^2 - r_m^2}{2r} \right| = \frac{\Delta p g_c}{L} R_H \quad (1)$$

where  $r_m$  is the radius at which the shearing stress is zero. If there is a solid boundary at the radius  $r_s$ , the absolute value of the skin friction is

$$\tau_s g_c = \frac{\Delta p g_c}{L} \left| \frac{r_s^2 - r_m^2}{2r_s} \right| = \frac{\Delta p g_c}{L} R_{Hs} \quad (2)$$

If the pressure gradient is independent of the radial position, the shearing stress is obviously linear in the hydraulic radius  $R_H$  written on the portion of the stream between the radius of zero shear and the radius where the shearing stress is measured. The profile of the shearing stress is unaffected by the type of flow and the equations are equally valid for laminar or turbulent motion.

#### DISTRIBUTION OF VELOCITY

The relationship between the shearing stress and velocity gradient on the time-average basis can be expressed as

$$\tau g_c = -(\mu + \epsilon) \frac{du}{dr} \quad (3)$$

The eddy viscosity  $\epsilon$  is best taken to be simply a parameter accounting for nonlaminar stresses. If  $\epsilon$  is to be zero or positive, the radius of zero shear  $r_m$  must also be the radius of maximum velocity. Brighton and Jones have confirmed this experimentally (1).

When the eddy viscosity is expressed in terms of the local velocity, Equations (1), (2), and (3) can be combined and integrated between  $r_s$  and  $r$  or  $r_m$  as the case may be. It is convenient to introduce the average of  $\epsilon$  taken on the velocity  $u$  over the portion of the stream covered by the integration. By calling the average  $\epsilon^o$ , the integral equation for the portion between  $r_s$  and  $r$  is

$$\frac{\left(1 + \frac{\epsilon^o}{\mu}\right) u}{R_{Hs} \tau_s g_c / \mu} = \frac{1}{2} \left[ \frac{1}{2R_{Hs}^2} \left( r_s^2 - r^2 - 2r_m^2 \ln \frac{r_s}{r} \right) \right] = \frac{1}{2} \Phi_s \quad (4)$$

Similarly, over the whole distance between  $r_s$  and  $r_m$

$$\frac{\left(1 + \frac{\epsilon_m^o}{\mu}\right) u_m}{R_{Hs} \tau_s g_c / \mu} = \frac{1}{2} \left[ \frac{1}{2R_{Hs}^2} \left( r_s^2 - r_m^2 - 2r_m^2 \ln \frac{r_s}{r_m} \right) \right] = \frac{1}{2} \Phi_{ms} \quad (5)$$

For a tube,  $\Phi_{ms} = 2$  and  $(\Phi/\Phi_m)_s = 1 - (r/r_o)^2$ ; for parallel plates with half-clearance  $b$ ,  $\Phi_{ms} = 1$  and  $(\Phi/\Phi_m)_s = 1 - (r/b)^2$ .

Combining Equations (4) and (5), one obtains

$$\frac{\left(1 + \frac{\epsilon^o}{\mu}\right) u}{\Phi_s R_{Hs} \tau_s g_c / \mu} = \frac{1}{2} = \frac{\left(1 + \frac{\epsilon_m^o}{\mu}\right) u_m}{\Phi_{ms} R_{Hs} \tau_s g_c / \mu} \quad (6)$$

Within a given stream, the reduced velocity profile is

$$\frac{u}{u_m} = \left( \frac{\Phi}{\Phi_m} \right)_s \frac{\left(1 + \frac{\epsilon_m^o}{\mu}\right)}{\left(1 + \frac{\epsilon^o}{\mu}\right)} \quad (7)$$

and if the flow is everywhere laminar, then, of course

$$\frac{u}{u_m} = \left( \frac{\Phi}{\Phi_m} \right)_s \quad (8)$$

Equation (8) is simply a concise form of the usual laminar equation and it proceeds to the proper limits of parabolic flow for tubes and parallel plates.

#### CONDITIONS OF COMPARISON

It is convenient to define a Reynolds number for annular flow as

$$N_{Res} = 2 \Phi_{ms} R_{Hs} V \rho / \mu \quad (9)$$

This reduces to the usual Reynolds number for tube flow when  $r_1/r_2 = 0$ . It is also appropriate to define the Fanning friction factor at either surface of the annulus in the usual manner, namely

$$\tau_s g_c = (f_s/2) \rho V^2 \quad (10)$$

With these substitutions, the right-hand side of Equation (6) becomes

$$\left(1 + \frac{\epsilon_m^o}{\mu}\right) = \frac{1}{4} (N_{Res} \sqrt{f_s}) \left( \sqrt{f_s} \frac{V}{u_m} \right) \quad (11)$$

When one smooth tube is compared with another, it is well known that the reduced velocity profiles are coincident when  $\left(1 + \frac{\epsilon^o}{\mu}\right)$  is the same. In other words  $u/u_m$  in Equation (7) is a particular function of  $(\Phi/\Phi_m)_s$  alone. This suggests that coincident reduced profiles may be found in annuli of any diameter ratios provided they are compared at equal  $\left(1 + \frac{\epsilon_m^o}{\mu}\right)$ . If, in addition, the maximum velocity is held constant, coincidence of the absolute local velocities should result.

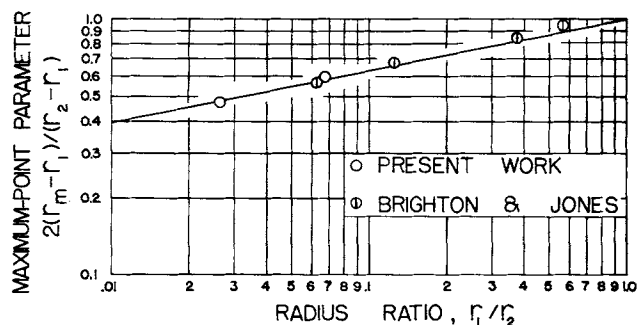


Fig. 1. Position of maximum point in annuli at high Reynolds numbers.

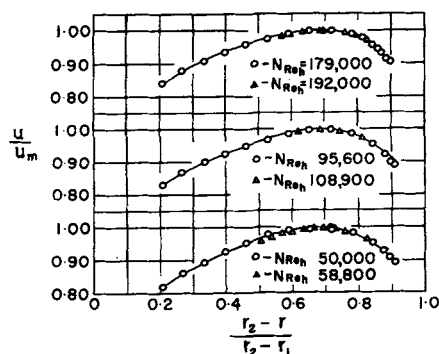


Fig. 2. Comparison of predicted and experimental velocities in the annulus with radius ratio of 14.8 (solid line indicates predicted profile).

Equation (11) indicates that the stated criteria are met whenever

$$\sqrt{f_s} (V/u_m) = \text{constant} \quad (12)$$

and

$$N_{Re_s} \sqrt{f_s} \propto N_{Re_s} (u_m/V) = \text{constant} \quad (13)$$

and

$$u_m = \text{constant} \quad (14)$$

The last three equations summarize the conditions of comparison adopted in the present work. Taken together they assert that equal local velocities occur in smooth annuli at equal values of  $(\Phi/\Phi_m)_s$  whenever the maximum velocity, the friction velocity, and the Reynolds number based on the maximum velocity are separately equal.

### RADIUS OF MAXIMUM VELOCITY

When the annular flow is wholly laminar, the maximum point is situated at the radius:

$$(r_m)_L = [(r_2^2 - r_1^2)/2 \ln (r_2/r_1)]^{1/2} \quad (15)$$

where  $r_1$  and  $r_2$  are the inner and outer radii of the annulus, respectively. The corresponding ratio of the skin frictions is

$$\left( \frac{\tau_1 g_c}{\tau_2 g_c} \right)_L = \frac{r_2}{r_1} \left[ \frac{(r_m)_L^2 - r_1^2}{r_2^2 - (r_m)_L^2} \right] = \frac{(R_{H1})_L}{(R_{H2})_L} \quad (16)$$

The subscript  $L$  is simply a reminder that the radius of maximum velocity has its laminar value. Equation (16) is equally valid for turbulent flow provided the maximum point happens to be at the laminar position.

In turbulent flow, the radius of maximum velocity depends on both the annular size and the Reynolds number. In general, the maximum point moves inward toward the core as the Reynolds number is increased. Although the influence of Reynolds number is greatest in the lower turbulent range, the maximum point is not far from  $(r_m)_L$  on the average. In the higher turbulent range, on the other hand, the maximum point is almost independent of the Reynolds number but the radius of maximum velocity is considerably less than the laminar value. The data of Brighton and Jones (1) indicate that at high Reynolds numbers

$$\frac{2(r_m - r_1)}{(r_2 - r_1)} = \left( \frac{r_1}{r_2} \right)^{0.20} \quad (17)$$

The ratio of skin frictions is

$$\frac{\tau_1 g_c}{\tau_2 g_c} = \frac{r_2}{r_1} \left( \frac{r_m^2 - r_1^2}{r_2^2 - r_m^2} \right) = \frac{R_{H1}}{R_{H2}} \quad (18)$$

It is useful to note that when the flow is entirely laminar, the skin frictions are related by the equation

$$(\Phi_{m1})_L (R_{H1})_L (\tau_1 g_c)_L = (\Phi_{m2})_L (R_{H2})_L (\tau_2 g_c)_L \quad (19)$$

which is merely Equation (6) applied to both the inner and outer portions of the stream simultaneously. There are no fully laminar situations involving a single fluid for which the radius of maximum velocity can be other than  $(r_m)_L$ . If the maximum point were at some other position such as  $r_m$ , say, the skin frictions would have to stand in a ratio different than the actual one. It is convenient, however, to imagine a hypothetical case of laminar flow in which the actual skin friction  $\tau_2 g_c$  is exerted at the outer surface and the maximum point is at  $r_m$  instead of  $(r_m)_L$ . This requires a fictitious skin friction  $(\tau_1 g_c)_F$  at the core such that

$$\Phi_{m1} R_{H1} (\tau_1 g_c)_F = \Phi_{m2} R_{H2} \tau_2 g_c \quad (20)$$

If the actual laminar flow is compared with the hypothetical laminar flow under the same skin friction at the outer wall, it follows that

$$\frac{(\tau_1 g_c)_L}{(\tau_1 g_c)_F} = \frac{(\Phi_{m2})_L (R_{H2})_L}{(\Phi_{m1})_L (R_{H1})_L} \left( \frac{\Phi_{m1} R_{H1}}{\Phi_{m2} R_{H2}} \right) \quad (21)$$

When the radius of maximum velocity is independent of the Reynolds number, the ratio of the actual and fictitious skin frictions at the core is therefore a function of the annular geometry alone. Consequently, Equation (21) is just as valid for turbulent flow at high Reynolds numbers as it is for laminar flow.

### COMPARISON OF TUBES AND ANNULI

#### Laminar Range

When purely laminar flow is considered, the proper choice of an equivalent tube is apparent from Equations (6), (8), and (19). In order to relate directly to the annulus, the tube should have the radius

$$r_o = (\Phi_{m2})_L (R_{H2})_L \quad (22)$$

and the skin friction

$$\tau_o g_c = (\tau_2 g_c)_L \quad (23)$$

Both the tube and the annulus carry the actual fluid. The Reynolds number of the annulus is

$$(N_{Re2})_L = \frac{2(\Phi_{m2})_L (R_{H2})_L V_a \rho_a}{\mu_a} \quad (24)$$

where the subscript  $a$  refers to the annulus as a whole.

The parabolic profile of velocity in the tube is immediately related to the annular profile through Equation (8). Under the conditions of comparison, the absolute local velocities are equal at equal values of the reduced distance parameter  $\Phi/\Phi_m$  since the maximum velocity is the same in the tube and annulus.

#### Lower Turbulent Range

Although the maximum point is influenced by the Reynolds number in the lower turbulent range, a rough approximation is sometimes adequate. On the average the maximum point is not far from the laminar position. When the radius of maximum velocity is  $(r_m)_L$ , it turns out that  $(\Phi_{m1})_L = (\Phi_{m2})_L$ . Therefore, as shown by Equation (6), the same tube operating at the same Reynolds number is equivalent to both the inner and outer portions of the annulus. The tube is exactly the one already described for laminar flow. Since the flow in this case is turbulent, however, the tube must be operated at a definite Reynolds

number. By virtue of Equation (12), the Reynolds number  $(N_{Re})_t$  of the equivalent tube is fixed by the condition

$$\frac{\tau_o g_c / \rho_a}{(\tau_2 g_c)_L / \rho_a} = 1 = \frac{f_t (V/u_m)_t^2}{(f_2)_L (V/u_m)_a^2} \quad (25)$$

where the subscript  $t$  refers to the tube. Since  $f_t$  and  $(V/u_m)_t$  for smooth tubes are functions of  $(N_{Re})_t$  alone, the tubular Reynolds number can be obtained from Equation (25) if  $(f_2)_L$  and  $(V/u_m)_a$  are known as functions of the annular Reynolds number  $(N_{Re2})_L$ .

If velocity data for tubes are available as graphs of  $(u/u_m)_t$  against  $(y/r_o)$  at constant Reynolds number, for example, the procedure is elementary. The reduced velocities  $(u/u_m)_t$  at the particular value of  $(N_{Re})_t$  obtained from Equation (25) are replotted against  $(\Phi/\Phi_m)_t$  where

$$\left( \frac{\Phi}{\Phi_m} \right)_t = \frac{y}{r_o} \left( 2 - \frac{y}{r_o} \right) \quad (26)$$

The resulting curve represents  $u/u_m$  against  $(\Phi/\Phi_m)_{2L}$  in the outer part of the annulus and  $u/u_m$  against  $(\Phi/\Phi_m)_{1L}$  in the inner part. It remains only to convert the  $(\Phi/\Phi_m)$  ratios to  $(r_2 - r)/(r_2 - r_1)$  by means of Equations (4) and (5) in order to obtain the reduced velocity profile in the annulus. The absolute local velocities are likewise coincident under the conditions of comparison.

#### Higher Turbulent Range

At high Reynolds numbers, the maximum point is essentially independent of the Reynolds number and is at the radius  $r_m$  shown in Equation (17) for all practical purposes. The actual skin friction at the outer wall of the annulus is  $\tau_2 g_c$  and the inner wall has the skin friction  $\tau_1 g_c$ .

Once more, the equivalent tube is exactly the same one whose radius is given by Equation (22) and whose skin friction is given by Equation (23). The tube again carries the actual fluid of density  $\rho_a$  and viscosity  $\mu_a$ . Since the maximum point in the annulus is not at the laminar position, however, the tube must be operated at one Reynolds number to be equivalent to the outer part of the annulus and at another to be equivalent to the inner part. In addition, to meet the criteria for comparison, the annulus must be imagined to carry different fluids on each side of the maximum point, neither of which is the actual fluid. The imaginary fluids can be thought of as having whatever properties are required to meet the conditions summarized in Equations (12), (13), and (14). The inner and outer parts of the annular stream must obviously be treated separately.

#### High Reynolds Number—Outer Portion

In order to meet the constraints placed on the comparison, the fluid flowing in the annulus can be imagined to have the actual density but a hypothetical viscosity. If the skin friction  $(\tau_2 g_c)_L$  of Equation (23) is set equal to the actual skin friction  $\tau_2 g_c$ , it follows that the equivalent tube must operate at such a Reynolds number  $(N_{Re})_t$  that

$$\frac{\tau_o g_c / \rho_a}{\tau_2 g_c / \rho_a} = 1 = \frac{f_t (V/u_m)_t^2}{f_2 (V/u_m)_a^2} \quad (27)$$

Strictly speaking, the proper Reynolds number  $N_{Re2}$  for the outer part of the annulus should be obtained from Equation (9) by using the actual value of  $r_m$  and the hypothetical viscosity of the fluid. An approximation avoids the need for such a calculation. Under the condition of Equation (13),  $N_{Re2}$  differs from  $(N_{Re2})_L$  only to the extent that  $(V/u_m)_a$  is affected by the shift of the maximum point from  $r_m$  to  $(r_m)_L$ . Since the change is very small, it is generally permissible to consider  $N_{Re2} =$

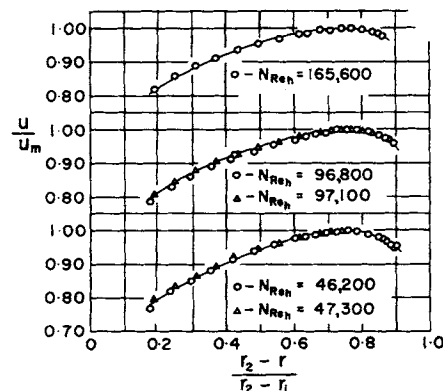


Fig. 3. Comparison of predicted and experimental velocities in the annulus with radius ratio of 38.2 (solid line indicates predicted profile).

$(N_{Re2})_L$ . Thus  $f_2$  and  $(V/u_m)_a$  measured in actual annuli can immediately be expressed as functions of  $(N_{Re2})_L$ , thus making them directly useful in Equation (27).

To obtain the reduced velocity,  $(N_{Re2})_L$  is computed and values of  $f_2$  and  $(V/u_m)_a$  are read at that Reynolds number. The Reynolds number  $(N_{Re})_t$  of the equivalent tube is obtained from tubular data and Equation (27). The relationship of  $(u/u_m)_t$  and  $(\Phi/\Phi_m)_t$  is also the relationship of  $u/u_m$  and  $(\Phi/\Phi_m)_2$  in the outer part of the annulus. It should be noted that the reduced distance parameter is obtained from Equations (4) and (5) with the radius of maximum velocity taken at its actual value  $r_m$  instead of  $(r_m)_L$ .

#### High Reynolds Number—Inner Portion

The inner part of the annulus must be imagined to carry a fluid with neither the density nor the viscosity of the actual one in order to meet the imposed constraints. In view of Equations (19) and (20), the hypothetical density  $\rho_a'$  must be such that

$$\frac{\tau_o g_c / \rho_a'}{\tau_2 g_c / \rho_a} = \frac{\tau_1 L g_c / \rho_a}{\tau_1 F g_c / \rho_a} = \frac{\tau_1 L g_c}{\tau_1 F g_c} \quad (28)$$

To be equivalent to the outer part of the annulus, the tube must operate at the Reynolds number  $(N_{Re})_t$ . To be equivalent to the inner part, it must operate at some other Reynolds number, say,  $(N_{Re})_p$ . By combining Equations (27) and (28), it can be seen that  $(N_{Re})_p$  must be such that

$$\frac{\tau_1 L g_c}{\tau_1 F g_c} = \frac{f_p (V/u_m)_p^2}{f_t (V/u_m)_t^2} \quad (29)$$

The skin friction ratio is obtained by means of Equation (21); the value of  $f_t (V/u_m)_t^2$  is known since  $(N_{Re})_t$  is known. Therefore, the Reynolds number  $(N_{Re})_p$  can be established directly. The relationship of  $(u/u_m)_t$  and  $(\Phi/\Phi_m)_t$  at  $(N_{Re})_p$  is also the relationship of  $u/u_m$  and  $(\Phi/\Phi_m)_1$  in the inner portion of the annulus. Again, the actual radius of maximum velocity  $r_m$  is used in computing  $(\Phi/\Phi_m)_1$ .

#### FRICTION FACTORS AND VELOCITY RATIOS

In the foregoing discussion, it has been assumed that the friction factor  $f_2$  and the velocity ratio  $(V/u_m)_a$  are readily available as functions of the working Reynolds number  $(N_{Re2})_L$ . When experimental data are not at hand, adequate values can be generated on the assumption that the tube forming the outer boundary of the annulus has the von Karman friction factor when no core is present. If such is the case

$$\frac{(V/u_m)_t}{\sqrt{f_2} (V/u_m)_a} = 1.738 \ln [(N_{Re})_t \sqrt{f_t}] - 0.40 \quad (30)$$

and

$$\frac{(V/u_m)_a}{(V/u_m)_t} = 1 + 1.738 \sqrt{f_t} \ln \left[ \frac{2}{(\Phi_{m2})_L} \right] \quad (31)$$

For a series of assumed values of  $(N_{Re})_t$ ,  $(V/u_m)_a$  can be obtained from Equation (31) and the Reynolds numbers  $(N_{Re2})_L$  can be calculated by means of Equation (13) on the assumption that  $N_{Re2}$  and  $(N_{Re2})_L$  are equal. Corresponding values of  $f_2$  can be calculated from Equation (30) and correlated with  $(N_{Re2})_L$ . Thus all of the information needed for the proposed method of solution are immediately available.

It should be recognized that the tubular Reynolds number  $(N_{Re})_p$  corresponding to the inner part of the annulus may be much greater than  $(N_{Re})_t$  corresponding to the outer part. Consequently, the best possible values of the tubular friction factor and velocity ratio over the whole range of Reynolds numbers should be used. At least Equation (30) should be replaced by actual data whenever possible. It is therefore highly desirable to obtain the friction factor  $f_t$  by running the outer pipe of the annulus without the core if it is at all feasible to do so.

## EXPERIMENTAL RUNS

Experimental velocity data were obtained in two vertical annuli 20 ft. long. The outer boundary was a smooth copper condenser tube with an I.D. of 0.760 in. The cores were smooth wires of iron-nickel alloy with diameters of 0.0515 and 0.0199 in. The radius ratios  $r_2/r_1$  were therefore 14.8 and 38.2. Both upward and downward flow were used and calming lengths of 100 and 200 outer tube diameters were available. The cores were centered under tension, so no supports were present to interfere with the flow. The test fluid was water flowing steadily at constant temperature.

Velocity profiles were obtained by means of impact probes made of stainless steel hypodermic tubing. The probes consisted of a bent 0.5-in. length of 0.035-in. O.D., 0.023-in. I.D. tubing silver soldered into a longer 0.065-in. O.D. tube to provide rigidity. The probes were moved across the stream by a feed mechanism sensitive to radial changes of 0.0002 in.

Impact pressures and static pressures were measured with manometers treated with silicone compound and by using water over fluorobenzene, water over chlorobenzene, water over mercury, and air over water. All manometers were read through a cathetometer with a precision of 0.05 mm. The impact probes were calibrated in place by the method of Stanton, Marshall, and Bryant (6).

Analysis of the data indicated that pressure drops and local main stream velocities in the turbulent range were obtained with the 2% precision usual in such work. Inspection of the confidence intervals at high Reynolds numbers indicated that the calibration error in the radius of maximum velocity was between 0.003 and 0.007 in., or something less than 2% of the clearance between the core and the outer tube. The radius of maximum velocity was established by fitting a polynomial to the experimental velocity data near the maximum and locating the maximum point of the polynomial once the data to be used and the degree of the polynomial had been determined analytically.

The outer tube was first operated without a core to establish its separate characteristics. Friction data were obtained at twenty-six Reynolds numbers between 8,000 and 572,000. Velocity profiles were measured at ten Reynolds numbers between 29,000 and 260,000.

The Reynolds number ranges investigated in the two annuli are most simply expressed in terms of the usual Reynolds number based on the overall hydraulic radius, namely

$$(N_{Re})_h = \frac{2(r_2 - r_1)V_a \rho_a}{\mu_a} \quad (32)$$

In the annulus with  $r_2/r_1 = 14.8$ , friction data were obtained at thirty-seven Reynolds numbers between 6,300 and 226,000. Velocity data were obtained at twenty-two Reynolds numbers between 760 and 222,000. In the annulus with  $r_2/r_1 = 38.2$ , friction data were taken at twenty-one Reynolds numbers between 8,100 and 198,000 and velocity data were obtained at twenty-three Reynolds numbers between 730 and 204,000.

## EXPERIMENTAL RESULTS

The data of Walker (7) and Croop (2) taken at radius ratios between 2.0 and 16.1 were reexamined, with polynomials to establish the maximum points. Inward movement of the maximum point with increased Reynolds number was confirmed in the lower turbulent range. Croop's data for  $r_2/r_1 = 16.1$  were in excellent agreement with those of the present work for  $r_2/r_1 = 14.8$  at Reynolds numbers  $800 \leq (N_{Re})_h \leq 10,000$ , the range in which the two sets of data overlapped. Above  $(N_{Re})_h = 30,000$  the maximum point showed little tendency to shift.

At high Reynolds numbers, the radii of maximum velocity were 0.132 in. for  $r_2/r_1 = 14.8$  and 0.098 in. for  $r_2/r_1 = 38.2$ , in excellent agreement with Equation (17). Figure 1 shows the comparison of the present data with the equation and with the data of Brighton and Jones (1).

The data obtained while running the outer tube without a core furnished values of the friction factors  $f_t$  and  $f_p$  and the velocity ratios  $(V/u_m)_t$  and  $(V/u_m)_p$  to be used in Equations (27) and (29). By means of these equations the reduced velocity profiles in the annuli were predicted at various Reynolds numbers and were compared with the experimental data as shown in Figures 2 and 3. It is apparent that the predicted profiles are in complete agreement with the data obtained in the experimental annuli.

To test the prediction at other radius ratios, comparisons were made with the notable data of Brighton and Jones as shown in Figure 4. Again the predicted profiles closely represent the actual experimental points. To complete the picture, eddy viscosities calculated from the

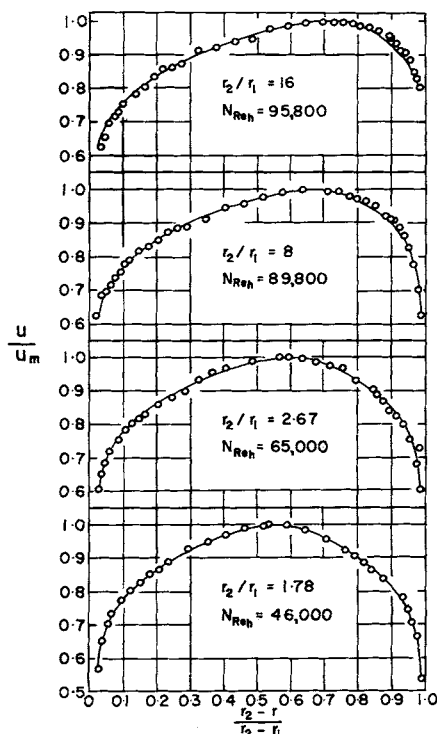


Fig. 4. Comparison of predicted velocities with the experimental data of Brighton and Jones (solid line indicates predicted profile).

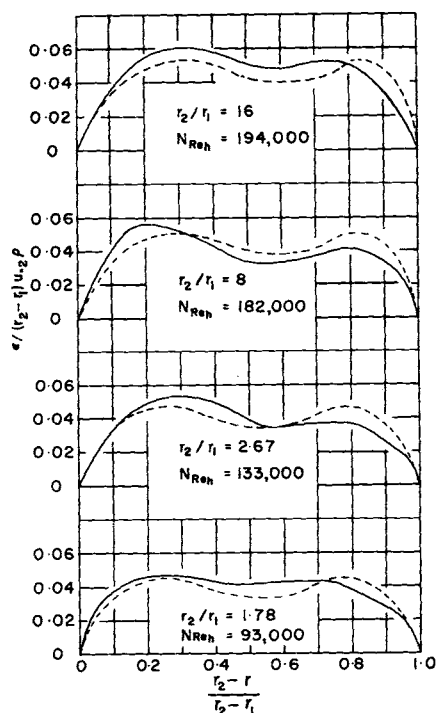


Fig. 5. Comparison of predicted eddy viscosities with experimental results of Brighton and Jones (solid line indicates experimental; broken line indicates predicted).

predicted velocity profiles are compared in Figure 5 with the experimental values measured by Brighton and Jones. Once more the agreement is excellent in view of the fact that the experimental values ordinarily scatter at least as much as the deviation between the curves.

When dealing with an annulus with a large ratio of outer to inner radii, the equivalent tube has a wide range of Reynolds numbers to cover. In order to meet that requirement and at the same time to provide a consistent set of tubular data for comparing the present work with that of Brighton and Jones, the reduced velocity profiles taken from Nikuradse's data (3) were used throughout. The predicted profiles of Figures 2, 3, and 4, therefore, have a common basis and their success in handling widely different radius ratios is not obscured by different sources of information. It can be concluded that the proposed method offers a most effective means of comparing tubes and annuli at high Reynolds numbers in order to establish annular velocity profiles from what is known about tubes.

#### ACKNOWLEDGMENT

The opportunity to carry out this development was granted to R. R. Rothfus by the Ford Foundation. W. K. Sartory received fellowship assistance from the National Science Foundation, the Minnesota Mining and Manufacturing Company, and the Stauffer Chemical Company.

The experimental part of the present work is based on a thesis submitted by Walter K. Sartory in partial fulfillment of the requirements for the degree of Doctor of Philosophy at Carnegie Institute of Technology. The thesis "Turbulent Flow in Annular Ducts" is available on interlibrary loan from the Hunt Library, Carnegie Institute of Technology, Pittsburgh, Pennsylvania 15213.

#### NOTATION

$f$  = Fanning friction factor at surface  $s$ , as defined by Equation (10), dimensionless  
 $g_c$  = conversion factor,  $32.2 \text{ (lb}_m\text{) (ft.) / (lb}_f\text{) (sec}^2\text{)}$

$L$  = length of ducts, ft.  
 $N_{Reh}$  = Reynolds number defined by Equation (32), dimensionless  
 $N_{Res}$  = Reynolds number defined by Equation (9), dimensionless  
 $N_{Ret}$ ,  $N_{Rep}$  = Reynolds numbers for tubes, dimensionless  
 $\Delta p$  = pressure drop due to friction,  $\text{lb}_f/\text{sq.ft.}$   
 $r$  = radial distance, ft.  
 $r_m$  = radius of maximum velocity, ft.  
 $r_o$  = radius of tube, ft.  
 $r_s$  = radius of surface  $s$ , ft.  
 $R_H$  = hydraulic radius defined by Equation (1), ft.  
 $R_{Hs}$  = hydraulic radius defined by Equation (2), ft.  
 $u$  = local fluid velocity, ft./sec.  
 $u_m$  = maximum local fluid velocity, ft./sec.  
 $u_*$  = friction velocity,  $(\tau_s g_c / \rho)^{1/2}$ , ft./sec.  
 $V$  = bulk average fluid velocity, ft./sec.  
 $y$  = distance from tube wall, ft.

#### Greek Letters

$\epsilon$  = local eddy viscosity,  $\text{lb}_m/(\text{sec.}) (\text{ft.})$   
 $\epsilon^o$  = average eddy viscosity taken on the local fluid velocity from  $r_s$  to  $r$ ,  $\text{lb}_m/(\text{sec.}) (\text{ft.})$   
 $\epsilon_m^o$  = average eddy viscosity taken on the local fluid velocity from  $r_s$  to  $r_m$ ,  $\text{lb}_m/(\text{sec.}) (\text{ft.})$   
 $\mu$  = viscosity of fluid,  $\text{lb}_m/(\text{sec.}) (\text{ft.})$   
 $\rho$  = density of fluid,  $\text{lb}_m/\text{cu.ft.}$   
 $\rho'$  = hypothetical fluid density in Equation (28),  $\text{lb}_m/\text{cu.ft.}$   
 $\tau$  = local shearing stress,  $\text{lb}_f/\text{sq.ft.}$   
 $\tau_o$  = skin friction at tube wall,  $\text{lb}_f/\text{sq.ft.}$   
 $\tau_s$  = skin friction at surface  $s$ ,  $\text{lb}_f/\text{sq.ft.}$   
 $\tau_{1L}$  = hypothetical skin friction defined by Equation (20),  $\text{lb}_f/\text{sq.ft.}$   
 $\Phi_s$  = local distance parameter defined by Equation (4), dimensionless  
 $\Phi_{ms}$  = maximum distance parameter defined by Equation (5), dimensionless

#### Subscripts

$a$  = annulus as a whole  
 $L$  = calculated as though the maximum point were at the laminar position regardless of its actual location  
 $m$  = position of zero shear or maximum local velocity  
 $p$  = flow in equivalent tube at the Reynolds number corresponding to the inner part of the annulus  
 $s$  = surface  $s$  or is on the same side of the maximum point as surface  $s$   
 $t$  = flow in equivalent tube at the Reynolds number corresponding to the outer part of the annulus  
 $1$  = inner surface of the annulus or the portion inside the maximum point  
 $2$  = outer surface of the annulus or the portion outside the maximum point

#### LITERATURE CITED

- Brighton, J. A., and J. B. Jones, *J. Basic Eng.*, **D86**, 835 (1964).
- Croop, E. J., Ph.D. thesis, Carnegie Inst. Technol., Pittsburgh, Pa. (1958).
- Nikuradse, J., *VDI-Forschungsheft*, **356**, 1 (1932).
- Rothfus, R. R., and C. C. Monrad, *Ind. Eng. Chem.*, **47**, 1144 (1955).
- Rothfus, R. R., J. E. Walker, and G. A. Whan, *A.I.Ch.E. J.*, **4**, 240 (1958).
- Stanton, T. E., D. Marshall, and C. N. Bryant, *Proc. Roy. Soc. (London)*, **A97**, 413 (1920).
- Walker, J. E., Ph.D. thesis, Carnegie Inst. Technol., Pittsburgh, Pa. (1956).

Manuscript received July 28, 1965; revision received April 25, 1966; paper accepted April 27, 1966.